Journal of Sustainable Development of Energy, Water and Environment Systems

http://www.sdewes.org/jsdewes

Year 2026, Volume 14, Issue 3, 1140713

Original Research Article

Life-Cycle Environmental Impacts of Residential Rooftop Photovoltaic Systems: A Case Study of Zagreb, Croatia

Jan Karl Ormuž, Irena Žmak*

Department of Materials, Faculty of Mechanical Engineering and Naval Architecture, University of Zagreb, Ivana Lučića 5, 10000 Zagreb, Croatia

e-mail: jan.ormuz@fsb.unizg.hr, irena.zmak@fsb.unizg.hr

Cite as: Ormuž, J. K., Žmak, I., Life Cycle Environmental Impacts of Residential Rooftop Photovoltaic Systems: A Case Study of Zagreb, Croatia, J.sustain. dev. energy water environ. syst., 14(3), 1140713, 2026,
DOI: https://doi.org/10.13044/j.sdewes.d14.0713

ABSTRACT

The environmental performance of residential rooftop photovoltaic electricity systems is becoming increasingly important for urban energy transition strategies. This study assesses whether rooftop photovoltaic electricity generation can reduce environmental impacts relative to conventional electricity supply in Zagreb, Croatia. It is hypothesised that rooftop photovoltaic electricity systems have lower climate-related and resource-related impacts than the national electricity grid mix. A screening cradle-to-use life cycle assessment was performed using site-specific electricity-generation data and impact categories defined by a European construction-product standard, with all impacts expressed per 1 kWh of electricity delivered. The results show a 65.89 per cent lower climate change impact and a 94 per cent lower fossil resource consumption than the modelled Croatian electricity grid mix. Overall, the findings suggest that rooftop photovoltaic systems in Zagreb can reduce climate and resource-related impacts under the assumed screening model.

KEYWORDS

Residential rooftop photovoltaics, Life cycle assessment, Environmental impacts, Electricity grid comparison, Croatia, OpenLCA.

INTRODUCTION

Addressing climate change remains a primary focus of European Union (EU) policies. The energy sector accounts for 27.4% of greenhouse gases [1]. Therefore, the EU has set the goal of achieving at least 42.5% of energy from renewables by 2030, with an aspiration to reach 45% [2]. Photovoltaic (PV) technology is cost-effective and easy to install. The Solar Energy Strategy targets 320 GW by 2025 and 600 GW by 2030, with initiatives to expedite PV permitting and mandate solar systems for new public, commercial, and residential buildings by 2029 [3]. Croatia, third among EU states, generated 73.7% of its net electricity from renewable energy sources [4], mainly hydro (47%) and wind (14.7%), with solar at 2.4% (2023) [5]. As hydro depends on water resources affected by climate change, Croatia is encouraged to diversify its energy sources [6].

Solar irradiation and space are the key criteria for photovoltaic (PV) implementation, unlike other renewables. Growing PV production and falling costs have accelerated the adoption of small and utility-scale systems. Real-time data-driven algorithms help evaluate financial viability amid market fluctuations. Agarwal *et al*. developed a greedy search

* Corresponding author

algorithm for high-capacity PV systems [7]. While large PV systems increase electricity output, they require extensive land, harming ecosystems and reducing arable land [8]. To mitigate this, research is shifting toward rooftop PV installations on urban buildings, which can help offset part of household electricity needs, reduce reliance on polluting grid power, and potentially improve energy security and lower costs. Optimal incentives for using roof space could maximise benefits, but more precise geographical data are needed to assess rooftop PV potential [9].

Residential rooftop photovoltaic systems have seen increasing adoption as a distributed energy solution contributing to decarbonisation and energy transition goals. Recent studies have examined various aspects of photovoltaic deployment, including diffusion dynamics of rooftop installations across different markets [10] and energy flow management in photovoltaic-based microgrids [11]. Furthermore, enhancing energy system performance is another crucial way to achieve sustainability, as properly cooled photovoltaic panels last longer and experience less performance loss [12]. Advanced cooling strategies using nanofluids can significantly mitigate thermal degradation, ensuring the system's performance remains stable throughout its service life [13]. These contributions highlight the focus on sustainable energy systems and provide a contextual foundation for assessing the environmental impacts of rooftop PV systems through life-cycle approaches.

Installing rooftop PV systems nationwide could meet 20–30% of electricity demand, as shown for the case of Spain [14]. A new method combining geographic information system (GIS), light detection and ranging (LiDAR), and cadastral data, applied to the district of Zaragoza, showed that dedicating 21% of available rooftop space to solar thermal can achieve domestic hot water self-sufficiency. Further, allocating the remaining suitable rooftop area to photovoltaic systems can achieve 20% electricity self-sufficiency under this prioritisation scenario [15]. Rooftop solar potential strongly depends on site-specific factors, such as climate. In the Netherlands, a bottom-up building-stock model (50% of renovated buildings and all new buildings) suggests that rooftop PV installations can potentially substitute 80% of public-grid electricity for appliances and lighting by 2050 [16]. In tropical climates like Puerto Rico, PV systems produce 2–3 times more energy than required, with excess supplied locally via the grid, reducing transmission losses [17].

Today, better management of electrical grid loads is needed to meet rising energy demand from new appliances and electric cars. PV-based electric vehicle (EV) charging systems and management schemes balance interactions among solar, batteries, and the grid, underscoring the need for integrated energy management to reduce grid stress and promote renewable energy use [18]. Proper energy management not only optimises energy flows but also directly enhances environmental quality by implementing energy-efficient processes [19]. Integrating rooftop PV and battery systems can reduce overloads and increase solar energy use, especially in rural low-voltage grids [20]. However, battery components use critical raw materials, raising environmental concerns like toxicity and resource scarcity [21]. Thus, ecological impacts, in addition to techno-economic benefits, must be considered when deploying rooftop PV systems.

Life cycle assessment is the primary method for evaluating the environmental impacts of rooftop PV systems throughout their lifespans. Tang *et al*. investigated potential reductions in household carbon dioxide (CO2) emissions under different rooftop PV configurations. They found PV systems with battery energy storage systems (BESS) to be optimal, though costly for most households. Conventional rooftop PV systems have slightly lower CO2 reduction but cost about a third as much, making them more practical [22]. Their energy payback time is 7 to 10 years, which is shorter than utility-scale systems [23]. Data on the carbon-reduction potential are inconclusive: some studies favour utility-scale PV systems [8], while others favour rooftop systems [24]. While greenhouse gases are a major concern, other environmental impacts are also important. Studies show that environmental performance depends on system design and life-cycle stage, complicating direct comparisons [25]. Additionally, numerous factors at different stages affect the environmental impact, most of which occur during module

production [26]. This impact can be lessened by relocating production to areas with higher renewable energy use [8]. End-of-life strategies, including waste transportation, also influence sustainability [27].

The environmental performance of rooftop PV systems is dependent on the installation location. Therefore, this study aims to assess the approximate environmental impacts of a case-study residential rooftop PV installation in Zagreb, Croatia, and compare them with those of an approximate reference of the Croatian grid mix.

The primary research inquiries are:

1. What is the estimated environmental impact of a rooftop photovoltaic (PV) system installed in Zagreb, Croatia?
2. How does the PV system's performance compare to the Croatian electrical grid in terms of environmental impact?

By answering these questions, this paper offers insights into whether residential rooftop PV systems can reduce selected life-cycle impacts, measured per the functional unit of 1 kWh, relative to the modelled Croatian electricity grid mix.

MATERIALS AND METHODS

Life cycle assessment (LCA) is a standardised method for evaluating the environmental impacts across different stages of a system's life cycle. It follows the framework outlined in the ISO 14040 and ISO 14044 standards, comprising four essential phases: defining the goal and scope, conducting a life-cycle inventory analysis, assessing impacts, and interpreting the findings [28], [29].

The study was presented as a screening, attributional, comparative LCA, as it compared two electricity-generating systems per functional unit using secondary and proxy-based inventory data, with the aim of identifying major impact patterns and hotspots rather than producing a product-specific environmental declaration.

The system boundaries were set as a cradle-to-use, excluding the end-of-life phase. For the PV system, this implies modelling of raw material extraction, upstream material processing, component manufacturing, transportation from the assumed country of origin to Zagreb, and electricity generation during the system's operational life. End-of-life treatment, including dismantling, waste transport, recycling, and disposal, was not considered due to a lack of consistent, detailed datasets across all components. Overall, the chosen system boundary represents a partial life-cycle model and should not be interpreted as a full cradle-to-grave assessment.

The functional unit was 1 kWh of electricity generated. All input and output flows, such as materials, energy, waste, and emissions, were allocated to this functional unit over the considered service life. The PV system lifetime was assumed to be 25 years, consistent with the commonly reported service lifetime of PV panels. Total lifetime electrical generation was estimated from the annual PV output, adjusted for module degradation.

The life-cycle model was developed using the open-source software OpenLCA. The rooftop PV system comprises PV modules, an inverter, a support structure, electrical cables, and associated transport processes. Access to commercial life-cycle inventory (LCI) databases was unavailable. Therefore, LCI data were compiled from freely available databases, including Tiangong and the European Reference Life-Cycle Database (ELCD), and supplemented with industry-reported life-cycle inventory data for PV technologies from the IEA PVPS (International Energy Agency Photovoltaic Power Systems Programme) Task 12 initiative [30]. Where an exact process dataset was unavailable, the closest available proxy process was selected based on material type, process function, and geographical and technological relevance. This approach was used to maintain model completeness, but it also introduces uncertainty. Foreground inventory data and proxy mappings used in the OpenLCA are provided in the Appendix (**Table A1**–**Table A6**).

Relative differences between the rooftop PV system and the Croatian electricity grid mix were calculated from the OpenLCA results for each impact category. Negative values indicate lower impacts for the PV system, whereas positive values indicate higher impacts. For categories in which the electricity grid result is zero or negative, no percentage comparison was reported because such values are not mathematically meaningful.

Life Cycle Assessment of a Photovoltaic System

A rooftop photovoltaic system is installed on a residential building in Zagreb, Croatia, covering an effective roof area of 50 m2. It includes 18 monocrystalline PV modules arranged in two strings of nine modules each, connected in series to the inverter. The modules are mounted on industry-standard rooftop structures.

The system is grid-connected and has a nominal installed capacity of 9.81 kWp (545 Wp per PV module). During design, the annual electrical energy consumption of a representative three-member household (two parents and one child), including daily electric vehicle charging, was considered, consistent with recent Croatian census data on average family size [31]. Figure 1 shows a schematic diagram of the installed photovoltaic system.

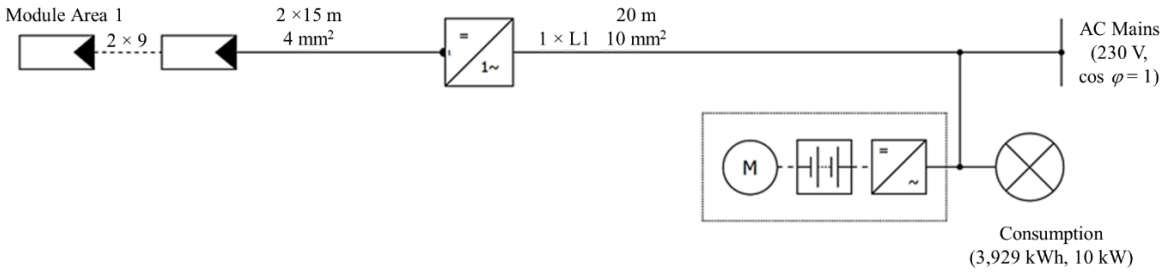

Figure 1. Schematic of a photovoltaic system with household appliances and one electric vehicle

The life-cycle inventory phase was conducted based on the number of components required for the PV system installation. Minor installation components, such as screws, nuts, and earthing cables, were not included because reliable quantity data were unavailable in the installation documentation. Their omission should therefore be interpreted as a foreground-data limitation of the present model rather than as evidence that these components are universally negligible. Furthermore, previous research supports this decision, as it found that the module production is the main contributor to the system's overall environmental impacts [26].

Photovoltaic Module

The photovoltaic module is the primary component of a photovoltaic (PV) system, generating environmentally sustainable electrical energy from solar irradiation. Although innovations in photovoltaic cell technology are introduced annually, silicon-based technologies continue to dominate the global photovoltaic market, a trend anticipated to endure until 2030 [32].

Conventional photovoltaic cell technology primarily comprises two categories: monocrystalline and polycrystalline, distinguished by differences in the manufacturing process for silicon wafers and the resulting crystalline structures. Wafers of both categories are doped with phosphorus and boron to establish a p-n junction. The interaction of photons with electron-hole pairs at this junction facilitates the generation of electrical current via the photoelectric effect, as illustrated in Figure 2 [33]. In terms of efficiency, monocrystalline PV cells often outperform polycrystalline cells, primarily due to higher material purity, a more uniform lattice structure, and fewer grain boundaries introduced by the Czochralski process. The inherent properties of silicon impose certain limitations on the maximum achievable

efficiency of this cell technology. Recent advancements, including the development of passivated emitter rear cell (PERC) technology, which employs a passivation layer at the rear of the cell to mitigate optical and recombination losses, have significantly enhanced cell efficiencies, bringing them closer to their theoretical maximum [34].

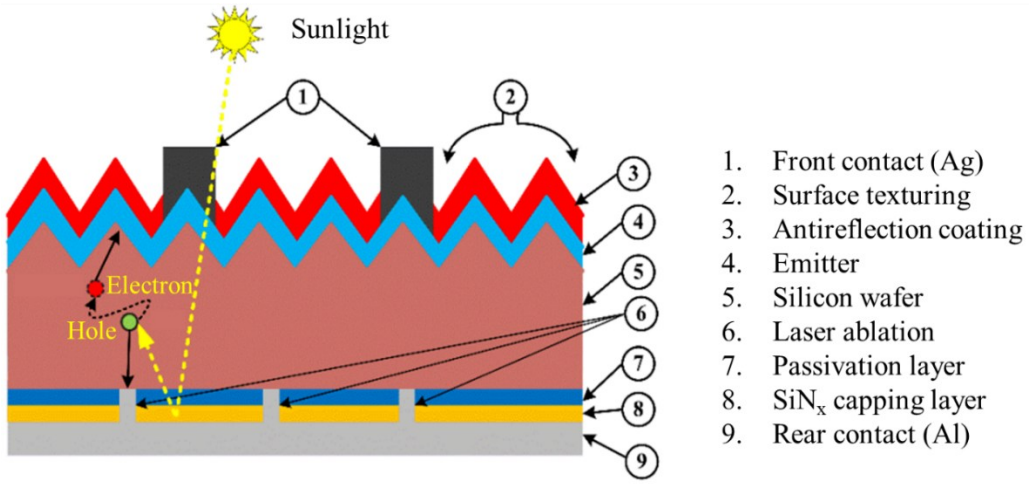

Figure 2. Structure of PERC solar cell [34]

Photovoltaic cells are vulnerable to mechanical damage and environmental degradation and require protection to last 25 years. Ethylene-vinyl acetate (EVA) acts as an encapsulant, securing the cells before enclosing them in the module frame, as shown in Figure 3. The module frame is made from aluminium alloys to lower transportation costs and preserve structural integrity. The back sheet provides support, while the tempered glass front cover ensures sufficient light transmission for energy conversion.

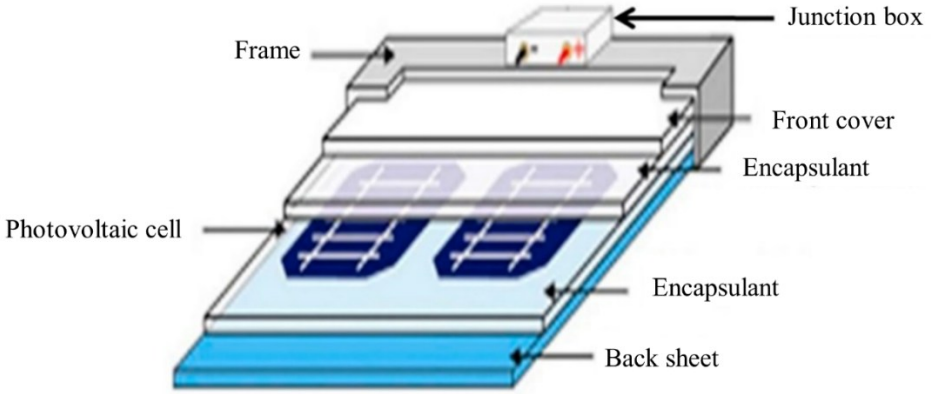

Figure 3. Monocrystalline silicon photovoltaic module [35]

Modules vary in shape, size, efficiency, and nominal power. Monocrystalline PERC-type module (Table 1) with a nominal power of 545 W and an efficiency of 21.09% is the main component of the PV system under study [36]. The choice of this specific module reflects the exact installed component at the case study's residential rooftop PV system installation location, rather than indicating that the study aims to compare PERC technology against alternative PV cell architectures. MPP refers to the maximum power point.

As manufacturer-specific LCI data for this exact product were not available, the module inventory was represented using adapted monocrystalline silicon PV manufacturing data from the IEA PVPS Task 12 dataset as the closest available proxy [30]. The module was linked to an assumed manufacturing location in China, the largest producer of silicon-based PV technologies, which accounts for 80% of the global supply [37]. Industrial partners validated

this assumption. The life cycle includes production steps such as refining metallurgical-grade silicon, using the Siemens or Czochralski process, cutting monocrystalline silicon wafers, manufacturing cells, and assembling modules.

When modelling the PV module life cycle in OpenLCA, upstream flows were matched to the best available proxies due to limited access to open-source, publicly available LCI databases.

Table 1. Technical specification of the studied PV [36]

Module RS545S8-144GA, Jiangsu Runda PV Co., Ltd., China			
MPP voltage [V]	41.92	Width [mm]	1134
MPP current [A]	13	Height [mm]	2279
Open circuit voltage [V]	50.04	Depth [mm]	30
Short circuit voltage [V]	13.84	Surface [m^2]	2.58
Nominal output [W]	545	Frame width [mm]	33
Fill factor [%]	78.69	Mass [kg]	32.5
Efficiency [%]	21.09		

Inverter

The direct current (DC) electrical power generated by photovoltaic (PV) modules from sunlight cannot be directly utilised in households or supplied to the grid. Consequently, it must be converted to alternating current (AC) power using an inverter to operate appliances, electric vehicles, and other electronic devices. Inverters are manufactured for various applications and are categorised by their maximum input power. Given that the installed PV system in Zagreb has a peak power of 9.81 kWp, a 10 kW inverter was selected. The Fronius Primo GEN24 inverter was chosen for this system based on its technical specifications, as detailed in **Table 2**. The selected commercial inverter was represented using a proxy life-cycle inventory for a representative European 10 kW inverter, based on IEA PVPS Task 12 LCI data [30]. Transport to Zagreb, Croatia, was assumed from the location of Fronius International's headquarters in Austria.

Table 2. Technical specification of the inverter Fronius Primo GEN24 (Fronius International) [38]

Fronius Primo GEN24 inverter, Fronius International, Austria			
Number of MPP trackers	2		
Max short circuit current, module array [A]	41.25 / 36	MPP voltage range $U_{MPP,min}$ to $U_{MPP,max}$ [V]	260–480
Max input current $I_{DC,max}$ [A]	22 / 22	Usable MPP voltage range [V]	65–480
Max PV input power [kW]	10.36	Number of DC connections	2 + 2
DC input voltage range $U_{DC,min}$ to $U_{DC,max}$ [V]	65–600	Nominal input voltage $U_{DC,r}$ [V]	400
Feed-in start voltage $U_{DC,start}$ [V]	80	Max PV generator power $P_{DC,max}$ [kWp]	15

Support Structures

Different PV systems require different mounting structures. For rooftop PV systems, modules are attached to an aluminium support structure and fixed with clamping elements, as shown in **Figure 4**. The assessment assumed that all support components were made of aluminium, either by extrusion or by sheet metal forming. The support was manufactured in Croatia, and cross-country transportation was included in the LCA assessment.

(a) (b)

Figure 4. Aluminium PV support structure (a); clamping system (b)

Electrical Cables

Two types of electrical cables are used in the PV system installation. PV arrays connect to the inverter via the H1Z2Z2-K single-core cable, a standard DC cable for solar power setups. This cable features a 4 mm2 cross-section copper wire that carries direct current. To prevent fire damage from short circuits, the copper wires are wrapped in low-smoke, zero-halogen polymer insulation, assumed to be polyethene for this study. Alternating current is supplied to the household via a five-core FG16OR 5×10 mm2 energy cable, which contains five copper conductors with polymer-based insulation and sheath materials. Because complete manufacturer-specific bill-of-material data were not available, the cable inventory was modelled using the dominant materials by mass, namely copper conductor and generic polymer insulation/sheath proxies. Electrical cables were assumed to be transported from Italy to the PV system installation site in Zagreb.

Photovoltaic System Electrical Energy Generation

Electrical generation from the rooftop PV system was simulated using PV*SOL software, based on the Metronom 8.2 dataset of hourly radiation (**Figure 5**) for the Maksimir neighbourhood in Zagreb, Croatia. The weather station is located at 45.81° north latitude and 16.03° east longitude, at an altitude of 112 metres. The annual global irradiation totals 1205 kWh/m2, with an average temperature of 12.6 °C. The PV system is mounted flush with the roof at a 30° tilt. Simulations used hourly data for a full year, resulting in a total annual electrical output of 11,871.82 kWh. Energy losses from transfer, conversion, and mismatches, as well as the overall system's energy balance, are shown in **Figure 6**.

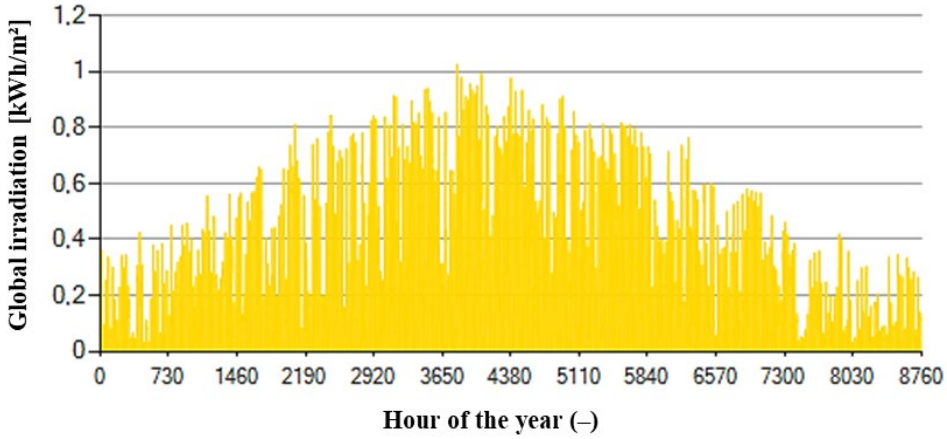

Figure 5. Hourly global radiation for Maksimir, Zagreb, Croatia (Metronom 8.2 dataset)

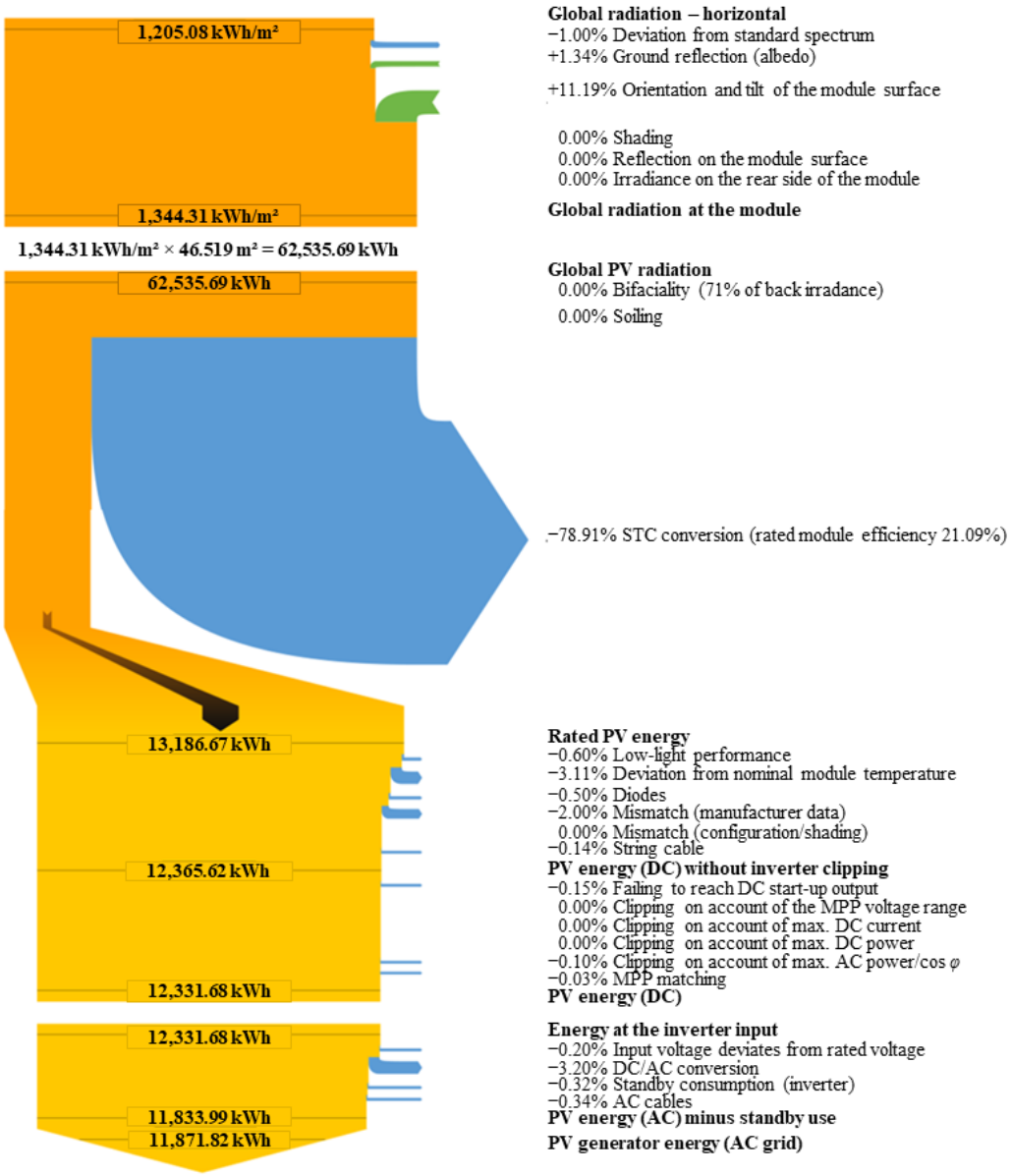

Figure 6. Energy balance Sankey diagram

The environmental impacts of power generation systems were evaluated using a functional unit of 1 kWh of electricity generated under the defined system boundaries. The PV system has an estimated lifespan of 25 years. Its total energy output was calculated by summing the annual PV generation, which was adjusted each year for module degradation at a rate of 0.5%:

$$E_{\mathrm{LC}} = E_1 \times (1 + \sum_{n=1}^{LC-1} (1 - n \times Deg) \quad (1)$$

where E_{LC} [kWh] is the energy produced through the lifespan, E_1 [kWh] is the annual energy production, *Deg* is the yearly module degradation factor, *n* is the module year used, and *LC* is the total lifespan of the module.

Life Cycle Assessment of the Electrical Grid Mix of Croatia

The PV system primarily aims to reduce environmental impacts, particularly greenhouse gas emissions. To assess its advantages, a life-cycle model of Croatia's electrical grid mix was developed for comparison. This model was built in OpenLCA (**Figure 7**) using publicly

available data on Croatia's various electricity sources shown in **Table 3** [5], [39], [40]. The Croatian electricity grid model was defined from cradle to electricity generation at the plant output, including upstream processes associated with fuel supply, material inputs, and electricity production. Because a specific Croatian national electricity grid inventory was not available in the accessible databases, each source was represented using the closest available regional or technology-specific background dataset.

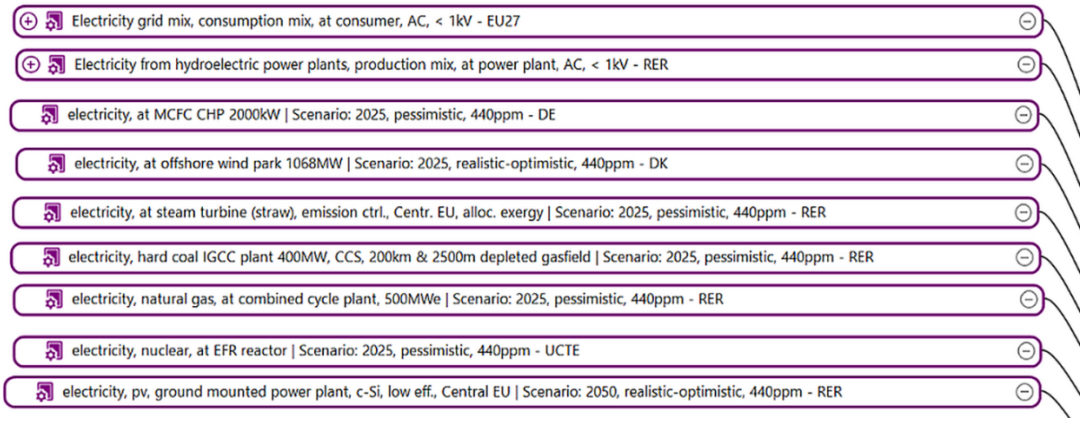

(a)

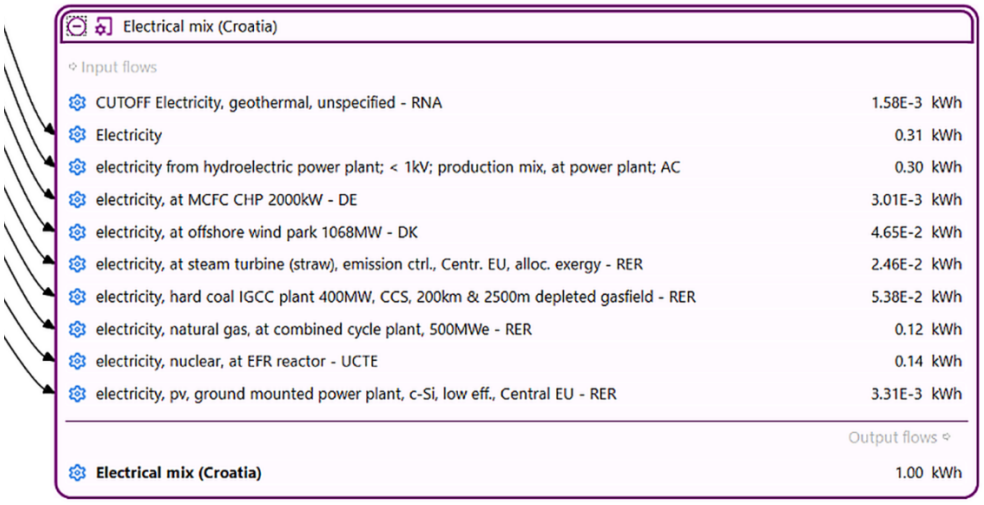

(b)

Figure 7. OpenLCA model of Croatia's electrical energy mix: upstream processes (a) and core process (b)

Table 3. Structure of electrical energy sources in Croatia [5], [39], [40]

Source of electrical energy	Share [%]	Subtype:	Sub-share [%]
Hydro	30.01		
Thermal – fossil	17.8	Fuel oil	1.68
		Natural gas	68.07
		Coal	30.23
Nuclear	13.68		
Renewable energy sources	7.6	Wind	61.24
		Solar	4.35
		Bio	32.34
		Geothermal	2.06
Total imports	30.91		

Electricity imports were approximated using the EU27 electricity mix; hydropower using a regional European average; fossil thermal generation using European background datasets for fuel oil, natural gas, and coal; and nuclear electricity using available European nuclear LCI data. Geothermal energy was excluded because of its negligible share in the reference electricity mix. A life-cycle impact assessment was performed in OpenLCA using the EN 15804+A2 impact categories, and results for both systems were reported on a per-functional-unit basis.

RESULTS AND DISCUSSION

A comparative assessment of the environmental impacts of a rooftop photovoltaic system installed in Zagreb was performed relative to the Croatian electricity grid mix. The life-cycle impact assessment was conducted for the environmental impact categories defined in EN 15804+A2, including climate change, acidification, resource depletion, and toxicity. All results (**Table 4**) were reported per 1 kWh of electricity generated, which is a common functional unit for power generation systems.

The rooftop PV system showed much lower climate change impacts than the modelled Croatian electricity grid mix, based on total emissions measured in terms of global warming potential (GWP) expressed as kg CO2-equivalent (kg CO2 eq.). Total climate change impact was 0.0285 kg CO2 eq. per kWh for the PV system and 0.0834 kg CO2 eq. per kWh for the electricity grid, corresponding to a 65.89% lower value for the PV system. This decrease was primarily due to the avoidance of direct fossil-fuel combustion in electricity generation. In both systems, the fossil subcategory dominated the overall results on climate change. The negative biogenic contribution in the electricity grid model can be attributed to biogenic-carbon accounting and data-specific characterisation, rather than from biomass combustion emissions.

The rooftop PV system also demonstrated significantly lower fossil fuel consumption than grid electricity, with a 94.58% reduction (0.0737 MJ for the PV system versus 1.3604 MJ for the grid). This showed that the modelled PV system can decrease fossil-fuel demand relative to the Croatian electricity grid, and that deploying similar systems in Zagreb could support the decarbonisation of Croatia's electricity sector.

Total human toxicity related to cancer was 64.52% higher for the PV system than for the grid, mainly because the organics subcategory had a significantly higher impact, whereas the metals subcategory had a lower impact. On the other hand, total human toxicity (non-cancer) was 52.56% lower for the PV system than for the electrical grid, with reductions observed across the inorganic, metal, and organic subcategories. These indicators are more sensitive to upstream dataset selection and proxy modelling choices than the core climate-change and fossil-resource results and should therefore be interpreted with greater caution.

The eutrophication impact results varied across subcategories between the PV system and the grid. Specifically, the rooftop PV system showed 78.43% lower freshwater eutrophication and 2.07% lower terrestrial eutrophication compared to the grid, but 4.59% higher marine eutrophication. This situation suggests that the relative environmental performance of the two systems depends on the emission pathways within each eutrophication subcategory, rather than on a single consistent trend.

Table 4. Environmental impact results for the rooftop PV system and the Croatian electricity grid mix

Impact category	PV system	Electricity grid mix – Croatia	Relative difference [%]
Acidification [mol H^+ eq.]	3.5841×10^{-4}	2.1531×10^{-4}	66.46
Climate change [kg CO_2 eq.]	2.8455×10^{-2}	8.3430×10^{-2}	−65.89
Climate change – Biogenic [kg CO_2 eq.]	1.4506×10^{-4}	-4.5130×10^{-4}	net-neg. grid
Climate change – Fossil [kg CO_2 eq.]	2.8310×10^{-2}	8.3881×10^{-2}	−66.25

Impact category	PV system	Electricity grid mix – Croatia	Relative difference [%]
Climate change – Land use and LU change [kg CO_2 eq.]	0	0	—
Ecotoxicity, freshwater [CTUe]	3.4636×10^{-2}	0.5442	−93.64
Ecotoxicity, freshwater – inorganics [CTUe]	1.2796×10^{-2}	4.2316×10^{-2}	−69.76
Ecotoxicity, freshwater – metals [CTUe]	2.0901×10^{-2}	0.48082	−95.65
Ecotoxicity, freshwater – organics [CTUe]	1.0439×10^{-3}	2.2705×10^{-2}	−95.40
Eutrophication, freshwater [kg P eq.]	4.8939×10^{-8}	2.2685×10^{-7}	−78.43
Eutrophication, marine [kg N eq.]	5.0728×10^{-5}	4.8504×10^{-5}	4.59
Eutrophication, terrestrial [mol N eq.]	5.3646×10^{-4}	5.4778×10^{-4}	−2.07
Human toxicity, cancer [CTUh]	1.6027×10^{-11}	9.7419×10^{-12}	64.52
Human toxicity, cancer – inorganics [CTUh]	4.4217×10^{-24}	0	—
Human toxicity, cancer – metals [CTUh]	1.0230×10^{-12}	7.4159×10^{-12}	−86.21
Human toxicity, cancer – organics [CTUh]	1.5004×10^{-11}	2.326×10^{-12}	545.05
Human toxicity, non-cancer [CTUh]	1.7612×10^{-10}	3.7122×10^{-10}	−52.56
Human toxicity, non-cancer – inorganics [CTUh]	6.7059×10^{-12}	7.08×10^{-11}	−90.55
Human toxicity, non-cancer – metals [CTUh]	1.6788×10^{-10}	3.2208×10^{-10}	−47.88
Human toxicity, non-cancer – organics [CTUh]	1.9313×10^{-12}	1.3858×10^{-11}	−86.06
Ionising radiation [kBq U-235 eq.]	4.4195×10^{-4}	2.0868×10^{-2}	−97.88
Land use [Pt]	5.1232×10^{-3}	6.5351×10^{-2}	−92.16
Ozone depletion [kg CFC11 eq.]	5.3429×10^{-10}	8.9973×10^{-9}	−94.06
Particulate matter [disease incidence]	1.9976×10^{-9}	1.0502×10^{-9}	90.21
Photochemical ozone formation [kg NMVOC eq.]	1.5547×10^{-4}	1.5922×10^{-4}	−2.36
Resource use, fossils [MJ]	7.3708×10^{-2}	1.3605	−94.58
Resource use, minerals and metals [kg Sb eq.]	2.7414×10^{-9}	2.0124×10^{-8}	−86.38
Water use [m^3 deprivation]	24.539	–8.0738	net-neg. grid

Freshwater ecotoxicity was lower for the rooftop PV system than for the electrical grid in the current model. Total freshwater ecotoxicity was 3.4636×10−2 CTUe for the PV system and 5.4422×10−1 CTUe for the grid, representing a 93.64% reduction for the PV system. The PV system also exhibited lower results in the inorganic, metal, and organic freshwater ecotoxicity subcategories. Since ecotoxicity indicators remain sensitive to the underlying background datasets, these results should still be viewed as model-dependent, rather than manufacturer-specific.

The lower ionising-radiation indicator for the PV system compared to the Croatian grid was primarily due to the inclusion of nuclear-generated electricity in the Croatian grid mix, which comes from the Slovenian-Croatian Krško nuclear power plant.

Regarding land use, the grid mix showed a higher value (0.0654 Pt) than the rooftop PV system (0.0051 Pt). This result is consistent with the use of existing roof space for PV installations. The rooftop PV system had an ozone-depleting potential that is 94% lower than that of the grid model. It also showed a slightly lower photochemical ozone formation indicator than the electrical grid, namely by 2.36%. On the other hand, the particulate matter indicator was higher for the rooftop PV system. These categories are likely influenced by upstream material manufacturing, processing, and transportation and should be understood as supply-chain-sensitive results within the current screening model.

The water-use category presents contrasting results between the two systems. The rooftop PV system shows a positive water-deprivation impact of 24.5 m3, mainly attributable to upstream manufacturing processes. In contrast, the Croatian electricity grid mix yields a net-negative water deprivation value (–8.07 m3), which can be attributed to methodological credits and regional water scarcity factors embedded in the life-cycle inventory data. Such a negative value indicates modelling assumptions, rather than physical water production and should therefore be interpreted with caution.

The results show that, based on the assumptions of this screening comparative LCA, the rooftop PV system in Zagreb, Croatia, can decrease selected environmental impact parameters, such as climate change, fossil resource use, ionising radiation, land use, ozone depletion, freshwater eutrophication, and freshwater ecotoxicity, compared to the modelled Croatian grid mix. Further enhancement of rooftop PV environmental performance will mainly rely on lower-impact upstream manufacturing, cleaner material supply chains, and the future incorporation of robust end-of-life recovery scenarios.

Overall, this screening and comparative LCA indicated that rooftop PV systems in Zagreb can lower life-cycle climate impacts and fossil resource demand per delivered kilowatt-hour compared to the modelled Croatian electricity grid mix.

LIMITATIONS

This study has several limitations that affect the interpretation of LCA results. The PV system life-cycle inventory was based on publicly accessible datasets and the best available proxies, rather than manufacturer-specific cradle-to-gate inventories, especially for modules and inverters. It is reasonable to expect that environmental impact results vary among photovoltaic manufacturers due to differences in electricity mix for production, manufacturing routes, material composition, transport distances, and module efficiency. The Croatian grid mix was modelled as a comparative reference using publicly available data on electricity sources and the closest available regional background datasets, rather than a fully country-specific national inventory. Another limitation of this comparative study is that the compared systems were not modelled to the same downstream delivery point, since the Croatian electricity grid model was represented only up to the plant output. In contrast, the PV system included the electricity output at the end of the inverter cable. This boundary mismatch is expected to have a minor influence on the overall results, but it remains a limitation of the comparison.

End-of-life treatment, dismantling, recycling, and disposal scenarios for PV components were excluded because consistent data were unavailable for all system components. Electricity generation from the rooftop PV system was not measured on-site but was simulated in PV*SOL using average meteorological data for Zagreb and the installed system specifications. The model further assumed a fixed module degradation rate over a 25-year service life, without explicit modelling of effects such as soiling, shading, and future changes in manufacturing supply chains

A formal sensitivity or uncertainty analysis was not performed in the present study. Therefore, the results should be regarded as a screening comparative case study only, with the highest robustness in the climate-change and fossil-resource indicators and greater uncertainty in toxicity- and emissions-sensitive categories. Future developments in manufacturing, recycling, or grid decarbonisation could significantly influence several impact categories.

CONCLUSION

This study applied a screening life cycle assessment to evaluate the environmental impact of a rooftop photovoltaic (PV) system installed in Zagreb, Croatia, compared with a modelled Croatian electricity grid reference. Electricity generation simulations were performed using PV*SOL, while life-cycle modelling of the PV system was conducted in OpenLCA. PV

system's environmental impacts were calculated for the impact categories defined in EN 15804+A2. The results were presented per 1 kWh of electricity generated, and the life cycle inventories for the compared systems were constructed using publicly available and proxy background datasets.

The results indicate that installing a rooftop PV system can reduce climate change-related impacts and fossil fuel depletion relative to the Croatian electrical grid mix under the assumptions of this screening cradle-to-use model. The impact of climate change was 65.89% lower than that of the modelled Croatian grid mix, while fossil resource consumption dropped by 94.58%. These results suggest that rooftop PV installations may aid in climate change mitigation and decrease reliance on fossil fuels in the electricity sector.

The results also indicate that not all impact categories improve. In the current PV system model compared to the grid, human toxicity (cancer) is higher, whereas human toxicity (non-cancer) is lower. More broadly, acidification, marine eutrophication, and particulate matter were higher for the rooftop PV system than for the grid reference. These categories are considered more sensitive to upstream manufacturing assumptions, proxy dataset selection, and modelling choices than the core climate change and fossil resource results and should therefore be interpreted with greater caution.

Overall, the study suggests that rooftop PV systems in Zagreb can lower life-cycle greenhouse gas emissions and fossil resource consumption per delivered kilowatt-hour compared to the modelled Croatian electricity grid mix. Nevertheless, the results of this screening, comparative life cycle assessment, should be taken with caution due to limitations in the available LCI datasets and the use of proxy processes in designing the LCA models of the two compared systems.

Future work should include end-of-life scenarios, improved national-grid inventory modelling, and the integration of BESS. These additions would provide a broader understanding of the life-cycle impacts of PV systems and of how energy management systems affect the environment.

NOMENCLATURE

Symbols

Deg	Yearly Module Degradation Factor	
E	Energy	[kWh]
I	Current	[A]
LC	Total Lifespan	[years]
n	Module Lifetime in Use	[years]
P	Power	[kW]
U	Voltage	[V]

Greek letters

φ	Phase Angle	[°]

Subscripts and superscripts

DC,max	Maximum Direct Current
DC,min	Minimum Direct Current
DC,r	Nominal Input Direct Current
DC,start	Start Direct Current
LC	Total Lifespan
MPP,max	Maximum Power Point, Maximum
MPP,min	Maximum Power Point, Minimum

Abbreviations

AC	Alternating Current
BESS	Battery Energy Storage System
CFC11 eq.	Trichlorofluoromethane Equivalent
CO_2 eq.	CO_2-Equivalent
CTUe	Comparative Toxic Unit for Ecosystems
CTUh	Comparative Toxic Unit for Humans
DC	Direct Current
EU	European Union
EU27	European Union 27 Member States
EV	Electric Vehicle
H^+ eq.	Hydrogen Ion Equivalent
IEA	International Energy Agency
ISO	International Organization for Standardization
kBq U-235 eq.	Ionising Radiation-Equivalent
LCA	Life Cycle Assessment
LCI	Life Cycle Inventory
LiDAR	Light Detection and Ranging
LU	Land Use
MPP	Maximum Power Point
N eq.	Nitrogen Equivalent
NMVOC eq.	Non-Methane Volatile Organic Compounds-Equivalent
P eq.	Phosphorus Equivalent
PERC	Passivated Emitter Rear Cell
Pt	Points
PV	Photovoltaic
PVPS	Photovoltaic Power Systems Programme
Sb eq.	Antimony-Equivalent
STC	Standard Test Conditions

REFERENCES

1. European Parliament, Greenhouse gas emissions by country and sector (infographic), https://www.europarl.europa.eu/topics/en/article/20180301STO98928/greenhouse-gas-emissions-by-country-and-sector-infographic, [Accessed: Dec. 20, 2025].
2. European Parliament and Council, Directive (EU) 2023/2413 of the European Parliament and of the Council of 18 October 2023 amending Directive (EU) 2018/2001, Regulation (EU) 2018/1999 and Directive 98/70/EC as regards the promotion of energy from renewable sources, and repealing Council Directive (EU) 2015/652, https://eur-lex.europa.eu/eli/dir/2023/2413/oj/eng, [Accessed: Mar. 04, 2026].
3. European Commission, EU Solar Energy Strategy, https://eur-lex.europa.eu/legal-content/EN/TXT/?uri=celex:52022DC0221, [Accessed: Dec. 20, 2025].
4. Eurostat, Electricity from renewable sources reaches 47% in 2024, https://ec.europa.eu/eurostat/web/products-eurostat-news/w/ddn-20250319-1, [Accessed: Dec. 20, 2025].
5. The International Energy Agency, Energy system of Croatia, https://www.iea.org/countries/croatia, [Accessed: Dec. 20, 2025].
6. Ahialey, E. K., Kabo–Bah, A. T., and Gyamfi, S., Impacts of LULC and climate changes on hydropower generation and development: A systematic review, *Heliyon*, Vol. 9, No. 11, pp e21247, 2023, https://doi.org/10.1016/j.heliyon.2023.e21247.

7. Agarwal, U., Rathore, N. S., Jain, N., Sharma, P., Bansal, R. C., Chouhan, M., and Kumawat, M., Adaptable pathway to net zero carbon: A case study for Techno-Economic & Environmental assessment of Rooftop Solar PV System, *Energy Rep.*, Vol. 9, pp 3482–3492, 2023, https://doi.org/10.1016/j.egyr.2023.02.030.
8. Brivio, E., Danelli, A., and Girardi, P., Ground-mounted or residential rooftop photovoltaic plant − European production or Chinese production: which is the most environmentally sustainable system? A case study in Italy, *EPJ Photovolt.*, Vol. 15, pp 8, 2024, https://doi.org/10.1051/epjpv/2024005.
9. Zhang, X., Walch, A., Rüdisüli, M., Bauer, C., Burgherr, P., McKenna, R., and Habert, G., Evaluating the levelized costs and life cycle greenhouse gas emissions of electricity generation from rooftop solar photovoltaics: a Swiss case study, *Environ. Res.-Infrastruct. Sustain.*, Vol. 4, No. 4, pp 045002, 2024, https://doi.org/10.1088/2634-4505/ad80c3.
10. Batista Da Silva, H., Thakur, J., Uturbey, W., and Martin, V., Analysis of residential rooftop photovoltaic diffusion in India through a Bass model approach, *J. Sustain. Dev. Energy Water Environ. Syst.*, Vol. 10, No. 4, pp 1–10, 2022, https://doi.org/10.13044/j.sdewes.d10.0423.
11. Dadjiogou, K. Z., Ajavon, A. S. A., and Bokovi, Y., Energy Flow Management in a Smart Microgrid Based on Photovoltaic Energy Supplying Multiple Loads, *J. Sustain. Dev. Energy Water Environ. Syst.*, Vol. 12, No. 1, pp 1–27, 2024, https://doi.org/10.13044/j.sdewes.d11.0473.
12. Hussein, S. M., Jafari, M., Taghi Shervani-Tabar, M., and Esmail Razavi, S., Numerical Investigation Into Photovoltaic (PV) Panel Performance Using a Hybrid Nanofluid Cooling Approach, *Transactions of FAMENA*, Vol. 48, No. 4, pp 65–86, 2024, https://doi.org/10.21278/TOF.484065624.
13. Muniyandi, S. and Narayanasamy, S., Experimental analysis on the performance of photovoltaic module with Al2O3 deionized water nanofluid, *Therm. Sci.*, Vol. 28, No. 1 Part A, pp 357–364, 2024, https://doi.org/10.2298/TSCI230829268M.
14. Jiménez-Castillo, G., Martínez-Calahorro, A. J., Rus-Casas, C., Snytko, A., and Muñoz-Rodríguez, F. J., Performance analysis indices for Rooftop Solar Photovoltaic system, *IEEE Latin Am. Trans.*, Vol. 21, No. 9, pp 999–1006, 2023, https://doi.org/10.1109/TLA.2023.10251806.
15. Guillén-Lambea, S., Sierra-Pérez, J., García-Pérez, S., Montealegre, A. L., and Monzón-Chavarrías, M., Energy Self-Sufficiency Urban Module (ESSUM): GIS-LCA-based multi-criteria methodology to analyze the urban potential of solar energy generation and its environmental implications, *Sci. Total Environ.*, Vol. 879, pp 163077, 2023, https://doi.org/10.1016/j.scitotenv.2023.163077.
16. Yang, X., Hu, M., Tukker, A., Zhang, C., Huo, T., and Steubing, B., A bottom-up dynamic building stock model for residential energy transition: A case study for the Netherlands, *Appl. Energy*, Vol. 306, pp 118060, 2022, https://doi.org/10.1016/j.apenergy.2021.118060.
17. Bozzo-Vazquez, A., Carrero-Garcia, A., Del-Valle-Nieves, G., Galarza-Molares, N. E., Goenaga-Buelvas, S. A., and Goenaga-Jimenez, M. A., Study of Photovoltaic Array Implementation on Residential Roofs in Puerto Rico, *2023 IEEE PES Innovative Smart Grid Technologies Latin America (ISGT-LA)*, San Juan, PR, USA, pp 140–144, November 6-9, 2023, https://doi.org/10.1109/ISGT-LA56058.2023.10328259.
18. Syafii, S., Krismadinata, K., Muladi, M., Agung, T. K., and Ananta Sandri, D., Simple Photovoltaic Electric Vehicles Charging Management System Considering Sun Availability Time, *J. Sustain. Dev. Energy Water Environ. Syst.*, Vol. 12, No. 1, pp 1–12, 2024, https://doi.org/10.13044/j.sdewes.d11.0476.

19. Tosanic, M., Miladinovic, D., Maksimovic, R., and Vidicki, P., Energy Performance Indicators in a Large Electrical Company, *Transactions of FAMENA*, Vol. 49, No. 3, pp 49–60, 2025, https://doi.org/10.21278/TOF.493051623.
20. Reibsch, R., Blechinger, P., and Kowal, J., The importance of battery storage systems in reducing grid issues in sector-coupled and renewable low-voltage grids, *J. Energy Storage*, Vol. 72, pp 108726, 2023, https://doi.org/10.1016/j.est.2023.108726.
21. Malode, S., Prakash, R., and Mohanta, J. C., Sustainability assessment of rooftop solar photovoltaic systems: A case study, *Environ. Impact Assess. Rev.*, Vol. 108, pp 107609, 2024, https://doi.org/10.1016/j.eiar.2024.107609.
22. Tang, Y., Cockerill, T. T., Pimm, A. J., and Yuan, X., Environmental and economic impact of household energy systems with storage in the UK, *Energy Build.*, Vol. 250, pp 111304, 2021, https://doi.org/10.1016/j.enbuild.2021.111304.
23. Ahmad Ludin, N., Ahmad Affandi, N. A., Purvis-Roberts, K., Ahmad, A., Ibrahim, M. A., Sopian, K., and Jusoh, S., Environmental Impact and Levelised Cost of Energy Analysis of Solar Photovoltaic Systems in Selected Asia Pacific Region: A Cradle-to-Grave Approach, *Sustainability*, Vol. 13, No. 1, pp 396, 2021, https://doi.org/10.3390/su13010396.
24. Roy, R. and Pearce, J. M., Is small or big solar better for the environment? Comparative life cycle assessment of solar photovoltaic rooftop vs. ground-mounted systems, *Int. J. Life Cycle Assess.*, Vol. 29, No. 3, pp 516–536, 2024, https://doi.org/10.1007/s11367-023-02254-x.
25. Roselli, C., Tariello, F., and Sasso, M., Integration of a Photovoltaic System with an Electric Heat Pump and Electrical Energy Storage Serving an Office Building, *J. Sustain. Dev. Energy Water Environ. Syst.*, Vol. 7, No. 2, pp 213–228, 2019, https://doi.org/10.13044/j.sdewes.d6.0248.
26. Abuzaid, H. and Samara, F., Environmental and Economic Impact Assessments of a Photovoltaic Rooftop System in the United Arab Emirates, *Energies*, Vol. 15, No. 22, pp 8765, 2022, https://doi.org/10.3390/en15228765.
27. Oteng, D., Zuo, J., and Sharifi, E., An evaluation of the impact framework for product stewardship on end-of-life solar photovoltaic modules: An environmental lifecycle assessment, *J. Clean Prod.*, Vol. 411, pp 137357, 2023, https://doi.org/10.1016/j.jclepro.2023.137357.
28. ISO 14044:2006, Environmental Management — Life Cycle Assessment — Requirements and Guidelines, International Organization for Standardization, Geneva, Switzerland.
29. ISO 14040:2006, Environmental Management — Life Cycle Assessment — Principles and Framework, International Organization for Standardization, Geneva, Switzerland.
30. Frischknech, R., Stolz, P., Krebs, L., de Wild-Scholten, M., Sinha, P., Fthenakis, V., Kim, H. C., Rauge, M., and Stucki, M., Life Cycle Inventories and Life Cycle Assessments of Photovoltaic Systems, (Technical) Report, IEA-PVPS T12-19:2020, Paris, France, 2020, https://iea-pvps.org/wp-content/uploads/2020/12/IEA-PVPS-LCI-report-2020.pdf, [Accessed: Feb. 01, 2026].
31. The number of divorces and one-person households grow, and the majority of families consist of a couple with one child, https://dzs.gov.hr/news/the-number-of-divorces-and-one-person-households-grow-and-the-majority-of-families-consist-of-a-couple-with-one-child/1611, [Accessed: Feb. 03, 2026].
32. Chowdhury, Md. S., Rahman, K. S., Chowdhury, T., Nuthammachot, N., Techato, K., Akhtaruzzaman, Md., Tiong, S. K., Sopian, K., and Amin, N., An overview of solar photovoltaic panels' end-of-life material recycling, *Energy Strateg. Rev.*, Vol. 27, pp 100431, 2020, https://doi.org/10.1016/j.esr.2019.100431.

33. Elfiky, S., Eliwa, A., Zahran, M., Kassem, A., and Farghal, A., A Study on the Impact of PN-Junction Doping Concentration on the Efficiency of Monocrystalline Silicon Solar Cells, *Sohag Eng. J.*, Vol. 3, No. 2, pp 165–177, 2023, https://doi.org/10.21608/sej.2023.224272.1041.
34. Kashyap, S., Madan, J., Pandey, R., and Sharma, R., Comprehensive Study on the Recent Development of PERC Solar Cell, *2020 47th IEEE Photovoltaic Specialists Conference (PVSC)*, Calgary, AB, Canada, pp 2542–2546, June 15 - August 21, 2020.
35. Gaddam, S. K., Pothu, R., and Boddula, R., Advanced polymer encapsulates for photovoltaic devices − A review, *J. Materiomics*, Vol. 7, No. 5, pp 920–928, 2021, https://doi.org/10.1016/j.jmat.2021.04.004.
36. Jiangsu Runda PV Co.,Ltd, Monocrystalline Module Half-cell Full Black Module, https://rundapv.com/products/perc/aurora/151.html, [Accessed: Feb. 13, 2026].
37. International Energy Agency (IEA), Special Report on Solar PV Global Supply Chains, (Technical) Report, Paris, France, 2022, https://doi.org/10.1787/9e8b0121-en.
38. Fronius, Fronius Primo GEN24 10.0, https://www.fronius.com/en/solar-energy/installers-partners/products/all-products/inverters/fronius-primo-gen24/fronius-primo-gen24-10-0, [Accessed: Dec. 20, 2025].
39. Vuk, B., Ban, M., Kos Grabar Robina, V., Golja, D., Milešević, B., Lončarević, Š., Dorototić, H., Živković, S., Alar, T., Židov, B., Borković, T., Krstulović, V., Matijašević, N., Maras, J., and Čop, T., Energy in Croatia 2022, Annual Energy Report, (Technical) Report, Energy Institute Hrvoje Požar, Zagreb, Croatia, 2023, https://eihp.hr/energija-u-hrvatskoj-godisnji-pregled-za-2022/, [Accessed: Dec. 20, 2025].
40. HEP Opskrba d.o.o, Electricity sources: Structure of electricity sources in 2024, https://hep.hr/opskrba/electricity-market/eletricity-market/electricity-sources/1474, [Accessed: Jan. 20, 2025].

APPENDIX

This appendix reports the foreground exchanges explicitly entered in the OpenLCA model for the rooftop photovoltaic system case study in Zagreb. The tables present the direct material, energy, transport and selected direct output flows defined in the foreground model, together with the linked proxy provider datasets used for each exchange. For readability, concise provider labels are shown here; the underlying linked processes remain unchanged from the exported model files. The appendix should therefore be interpreted as a foreground life-cycle inventory disclosure and proxy mapping, rather than a complete manufacturer-specific cradle-to-gate background inventory.

Components for which no reliable bill-of-material quantity or linked background dataset was available in the working model are not added retrospectively in this appendix. All quantities are reported exactly as modelled in the supplied process spreadsheets. Table S6 presents the installed-system quantities and their normalisation to the functional unit of 1 kWh, based on the modelled lifetime electricity output.

Table A1. Foreground life-cycle inventory of the photovoltaic module process (reference unit = 1 m^2); adapted from [30]

Flow	Process	Amount	Unit	Linked provider or note
Input	Aluminium sheet	2.13	kg	Aluminium sheet, production mix
Input	Copper wire	0.103	kg	Copper wire, market/technology mix
Input	Corrugated cardboard	0.763	kg	Corrugated cardboard, recycled paper route
Input	Diesel	0.009	MJ	Diesel mix at refinery
Input	Electricity	14	kWh	Electricity mix, Jiangsu
Input	Ethylene-vinyl acetate copolymer	0.875	kg	Ethylene-vinyl acetate copolymer
Input	Flat glass, uncoated	8.81	kg	Flat glass, uncoated, at plant
Input	Glass-fibre reinforced plastics	0.295	kg	Glass-fibre reinforced plastics
Input	Hydrogen fluoride	0.062	kg	Hydrogen fluoride proxy
Input	Isopropanol	0.147	g	Cut-off
Input	Lead (99.995%)	0.725	g	Lead, primary/secondary mix
Input	Organic silicone	0.122	kg	Organic silicone
Input	Photovoltaic cell, single-Si, at the plant	1	m^2	Foreground-linked process
Input	Polyethene high-density granulate (PE-HD)	0.024	kg	PE-HD granulate
Input	Polyethylene terephthalate	0.346	kg	Polyethylene terephthalate
Input	Potassium hydroxide	0.051	kg	Cut-off
Input	Recycled polyvinyl chloride	0.112	kg	Recycled polyvinyl chloride
Input	Soap	0.012	kg	Soap production proxy
Input	Tin rod	0.013	kg	Tin rod production proxy
Input	Transport in t·km	16.6	t·km	Road transport, small lorry
Input	Transport in t·km	2.77	t·km	Road transport, 32 t lorry
Input	Water, unspecified natural origin, CN	5.03	m^3	Direct
Input	Wooden pallet (EURO)	0.05	kg	Wooden pallet, EURO
Output	Carbon dioxide, fossil	0.022	kg	Direct elementary flow
Output	Heat, waste	50.3	MJ	Direct output
Output	NMVOC, unspecified origin	8.06	g	Direct elementary flow
Output	Water, CN	0.503	kg	Direct output
Reference product	Photovoltaic panel, single-Si, at plant	1	m^2	Reference flow

Table A2. Foreground life-cycle inventory of the delivered PV panel process (reference unit = 1 panel at the installation location)

Flow	Exchange flow	Amount	Unit	Linked provider or note
Input	Photovoltaic panel, single-Si, at the plant	2.58	m^2	Foreground-linked process
Input	Transport in t·km	7.833	t·km	Road transport, 22 t lorry
Input	Transport in t·km	543.9	t·km	Ocean freight, container ship
Input	Transport in t·km	0.455	t·km	Road transport, small lorry
Input	Transport in t·km	4.875	t·km	Rail transport, electric cargo
Reference product	PV panel at the location	1	Item(s)	Reference flow

Table A3. Foreground life-cycle inventory of the inverter process (reference unit = 1 inverter); adapted from [30]

Flow	Exchange flow	Amount	Unit	Linked provider or note
Input	Aluminium extrusion profile	12.23	kg	Aluminium extrusion profile, production mix
Input	Copper wire	4.9	kg	Copper wire, market/technology mix
Input	Corrugated board boxes	1.69	kg	Corrugated board boxes
Input	Cable/connector assembly	1	kg	Cable and connector proxy
Input	Glass-fibre reinforced plastics	0.066	kg	Glass-fibre reinforced plastics
Input	Ferrite	0.066	g	Iron oxide proxy
Input	Polyethene low-density foil (PE-LD)	0.029	kg	PE-LD foil
Input	Cold-rolled steel sheet	2.33	kg	Cold-rolled steel sheet
Input	Transformer	0.103	kg	Transformer production proxy
Input	Transport in t·km	52.1	t·km	Ocean freight, container ship
Input	Transport in t·km	5.79	t·km	Rail transport, diesel cargo
Input	Transport in t·km	1.736	t·km	Road transport, 22 t lorry
Output	Wastewater treatment flow	0.051	m^3	Direct output
Output	Heat, waste	97.5	MJ	Direct output
Output	Tap water	51	kg	Direct output
Output	Water, unspecified natural origin, DE	0.097	m^3	Direct output
Reference product	Inverter, 10 kW, average, at plant	1	Item(s)	Reference flow

Table A4. Foreground life-cycle inventory of the support-structure sub-processes

Component process	Reference unit	Exchange flow	Amount	Unit	Linked provider dataset
Aluminium channel	1 m	Aluminium sheet	0.418	kg	Aluminium sheet, production mix
Aluminium channel	1 m	Transport in t·km	0.018	t·km	Road transport, 22 t lorry
Aluminium channel cover	1 m	Aluminium sheet	0.163	kg	Aluminium sheet, production mix
Aluminium channel cover	1 m	Transport in t·km	0.007	t·km	Road transport, 22 t lorry
Aluminium extrusion profile	1 m	Aluminium extrusion profile	0.915	kg	Aluminium extrusion profile, production mix
Aluminium extrusion profile	1 m	Transport in t·km	0.040	t·km	Road transport, 22 t lorry
Aluminium end clamp	1 Item	Aluminium extrusion profile	0.031	kg	Aluminium extrusion profile, production mix
Aluminium end clamp	1 Item	Transport in t·km	0.001	t·km	Road transport, 22 t lorry
Aluminium mid clamp	1 Item	Aluminium extrusion profile	0.023	kg	Aluminium extrusion profile, production mix
Aluminium mid clamp	1 Item	Transport in t·km	0.001	t·km	Road transport, 22 t lorry

Table A5. Foreground life-cycle inventory of the cable sub-processes

Cable process	Reference unit	Exchange flow	Amount	Unit	Linked provider dataset
H1Z2Z2-K (1×4 mm^2)	1 m	Copper wire	0.044	kg	Copper wire, market/technology mix
H1Z2Z2-K (1×4 mm^2)	1 m	Polyethene high-density granulate (PE-HD)	0.020	kg	PE-HD production proxy
H1Z2Z2-K (1×4 mm^2)	1 m	Transport in t·km	0.028	t·km	Road transport, 22 t lorry
FG16OR16 (5×10 mm^2)	1 m	Copper wire	0.445	kg	Copper wire, consumption mix
FG16OR16 (5×10 mm^2)	1 m	Polypropylene granulate (PP)	0.048	kg	Polypropylene granulate
FG16OR16 (5×10 mm^2)	1 m	Polyurethane	0.197	kg	Direct
FG16OR16 (5×10 mm^2)	1 m	PVC resin (B-PVC)	0.083	kg	PVC resin, bulk polymerisation
FG16OR16 (5×10 mm^2)	1 m	Transport in t·km	0.342	t·km	Road transport, 22 t lorry

Table A6. Installed-system bill of materials and normalisation to the functional unit (1 kWh of electricity generated over the modelled lifetime)

System component	Quantity in the model	Unit	Linked foreground process	Quantity per 1 kWh
PV panel at the location	18	Item(s)	PV panel at the location	6.45×10^{-5}
Inverter	1	Item(s)	inverter, 10 kW, average, at the plant	3.59×10^{-6}
Aluminium extrusion profile	42	m	Aluminium extrusion profile	1.51×10^{-4}
Aluminium channel	40	m	Aluminium channel	1.43×10^{-4}
Aluminium channel cover	40	m	Aluminium channel cover	1.43×10^{-4}
Aluminium end clamp	12	Item(s)	Aluminium end clamp	4.30×10^{-5}
Aluminium mid clamp	30	Item(s)	Aluminium mid clamp	1.08×10^{-4}
FG16OR16 cable	20	m	FG16OR16 5 × 10 mm^2 + shipment from Italy	7.17×10^{-5}
H1Z2Z2-K cable	30	m	H1Z2Z2-K 1 × 4 mm^2 + shipment from Italy	1.08×10^{-4}
Reference output	278,898	kWh	Electrical energy production	1.00

Paper submitted: 22.12.2025
Paper revised: 27.03.2026
Paper accepted: 10.04.2026